Supporting Information

A Novel AIE-active imidazolium macrocyclic ratiometric fluorescence sensor for pyrophosphate anion

Jia-Bin Xiong[a,d,*], Ding-Ding Ban[a], Yong-Juan Zhou[a], Jin-Zhan Li[a], Si-Ru Chen[a], Guo-Qun Liu[a*], Jing-Jing Tian[c*], Li-Wei Mi[a*] and Dong-Mi Li[b*]

[a] School of Material and Chemical Engineering, Center for Advanced Materials Research, Zhongyuan University of Technology, Zhengzhou 450007, China;

[b] College of Chemistry and Chemical Engineering, Luoyang Normal University, Luoyang, Henan 471000, P.R. China,

[c] AIE Research Center, Shaanxi Key Laboratory of Phytochemistry, College of Chemistry and Chemical Engineering, Baoji University of Arts and Sciences, Baoji 721013, China.

[d] College of Chemistry, Green Catalysis Center, International Phosphorus Laboratory, International Joint Research Laboratory for Functional Organophosphorus Materials of Henan Province, Zhengzhou University, Zhengzhou 450001, People's Republic of China;

Materials: All reagents and solvents were chemical pure (CP) grade or analytical reagent (AR) grade and were used as received unless otherwise specified.

^{1}H NMR and ^{13}C NMR spectra were measured on a Bruker AV 400 spectrometer at 298 K in DMSO-d_6. Infrared spectra were recorded on BRUKER EQUINAX55 spectrometer. Absorption spectra were recorded on a Hewlett Packard 8453 UV–Vis spectrophotometer. Mass spectrum was measured on an IonSpec 4.7 Tesla FTMS instrument. Fluorescent emission spectra were collected on a Shimadzu RF-5301 fluorophotometer at 298 K.

Synthesis of the imidazolium macrocycle 1.

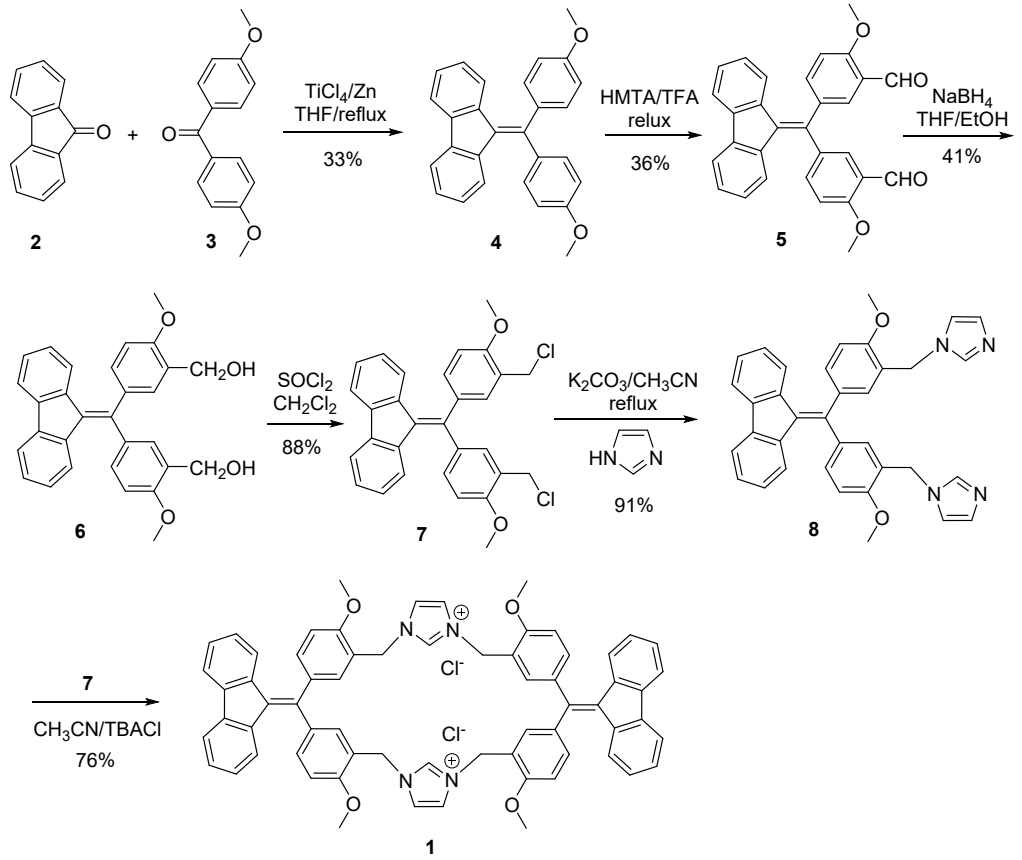

Scheme S1. Synthetic route of the imidazolium macrocycle **1**.

Preparation of the bridged TPE derivative 4: The preparation was carried out according to literature (*Adv. Mater.* 2011, 23, 3261–3265). To a flask equipped with a magnetic stirrer was charged with zinc dust (16 g, 160 mmol) and THF (100 mL) under nitrogen atmosphere. The mixture was cooled to 0 °C, and $TiCl_4$ (8.8 mL, 80 mmol) was added slowly by syringe. After the mixture was heated to reflux for 2.5 h, it was cooled to ambient temperature. Then 4,4'-dimethoxybenzophenone **3** and 9-fluorenone **2** (1:1.5 mole ratio, total 10 mmol) in THF (60 mL) was added, and the mixture was refluxed for 12 h. The reaction was quenched with 10% K_2CO_3 aqueous solution (100 mL) followed by extracting with dichloromethane. The organic layer was desiccated with anhydrous sodium sulfate, filtered, and evaporated to dryness under vacuum. The residue was purified by column chromatography to give yellow powders (1.3 g, 33%).

Preparation of dialdehyde 5: To a flask charged with **4** (1.0 g, 2.56 mmol), hexamethylenetetramine (3.58 g, 25.6 mmol) and tifluoroacetic acid (20 mL). The resultant mixture was refluxed under stirring for 30 min. After cooled to room temperature and quenched with 15 mL of water, the mixture was stirred for 4 h followed by extracting with dichloromethane (3 × 25 mL). The combined organic layer was desiccated with anhydrous sodium sulfate, filtered, evaporated to dryness under vacuum. The resultant slurry was purified with column chromatography to give orange red powders (410 mg, 36%).

Preparation of the dialcohol 6: To a flask was charged with **5** (410 mg, 0.92 mmol), $NaBH_4$ (350 mg, 9.19 mmol) and EtOH / THF (3: 2, V / V, total 25 mL). The mixture was stirred at ambient temperature for 3 h before it was washed with water and extracted with dichloromethane (3 × 25 mL). The combined organic phase was desiccated with anhydrous sodium sulfate, filtered, and evaporated to dryness under vacuum. The residue was subjected to column chromatography to give yellow powders (170 mg, 41%).

Preparation of the dichloride 7: To a flask was charged with **6** (180 mg, 0.4 mmol), pyridine (60 μL, 0.8 mmol) and 10 mL of dichloromethane. After stirred at room temperature for 10 min., a solution of $SOCl_2$ (0.17 mL) in dichloromethane (5 mL) was added dropwise over 30 min. The mixture was heated at 40 °C under stirring for 6 h before it was quenched and washed with water. The combined organic phase was desiccated with anhydrous sodium sulfate, filtered, and evaporated to dryness under vacuum. The residue was recrystallized with CH_2Cl_2 and MeOH to give yellow solids (172 mg, 88%).

Preparation of the diimidazole 8: To a flask was added **7** (96 mg, 0.2 mmol), imidazole (136 mg, 2 mmol), potassium carbonate (54 mg, 0.4 mmol), and redistilled CH_3CN (8 mL). After the mixture was refluxed under stirring for 5 h, it was cooled to room temperature, washed with water, and extracted with dichloromethane (3 × 15 mL). The combined organic layer was desiccated with anhydrous sodium sulfate, filtered, and evaporated to dryness under vacuum. The residue was purified by column chromatography to give yellow powders (100 mg, 91%). Mp: 204.3–205.7 °C; ^{1}H NMR (400 MHz, $CDCl_3$) δ (ppm) 7.58 (s, 2 H), 7.45 (s, 2 H), 7.23 (d, *J* = 8.6 Hz, 4 H), 7.09 (s, 2 H), 6.92 (s, 2 H), 6.91 (d, *J* = 8.6 Hz, 4 H), 6.78 (s, 4 H), 5.13 (s, 4 H), 3.87 (s, 6 H); ^{13}C NMR (100 MHz, CDCl3) δ (ppm) 160.2, 147.4, 140.0, 139.5, 137.4, 135.0, 132.0, 131.9, 129.8, 125.8, 125.0, 119.3, 118.2, 114.1, 55.3, 50.9; FTIR (KBr) *v* 3439, 2929, 1601, 1571, 1506, 1443, 1416, 1389, 1291, 1248, 1175, 1108, 1075, 1028, 906, 820, 737, 663, 630, 598 cm^{-1}; ESI$^+$ HRMS m/z calcd for $C_{36}H_{31}N_4O_2$ 551.2447 [M+H], found 551.2422 [M+H].

Preparation of the imidazolium macrocycle 1: To a flask was added **6** (106 mg, 0.19 mmol), **8** (94 mg, 0.19 mmol) and tetrabutylammonium chloride (268 mg, 0.96 mmol), and acetonitrile (8 mL). After the mixture was refluxed for 12 h under stirring and was cooled to room temperature, the resultant precipitates were collected by filtering and washed with dichloromethane to give red yellow powders (150 mg, 76%). Mp 251.4–253.2 °C; ^{1}H NMR (400 MHz, DMSO-d6) δ 9.36 (s, 2 H), 7.95 (s, 4 H), 7.81 (s, 4H), 7.24 (d, *J* = 8.0 Hz, 4 H), 7.20 (d, *J* = 8.4 Hz, 8 H), 7.04 (d, *J* = 8.8 Hz, 8 H), 6.67 (d, *J* = 8.4 Hz, 4 H), 5.41 (s, 8 H), 3.84 (s, 12 H); ^{13}C NMR (100 MHz, DMSO-d6) δ 159.8, 147.9, 139.6, 139.4, 139.1, 138.9, 135.7, 134.3, 133.2, 131.2, 131.0, 127.9, 123.9, 122.7, 120.7, 114.3, 55.2, 52.1; IR (KBr) *v* 3398, 3135, 3055, 3004, 2958, 2835, 1595, 1563, 1501, 1447, 1412, 1358, 1290, 1244, 1170, 1142, 1107, 1021, 966, 897, 819, 776, 732, 586, 537, 472 cm^{-1}; ESI+ HRMS m/z calcd for C66H54ClN4O4 1001.3833 [M-Cl], found1001.3835 [M-Cl].

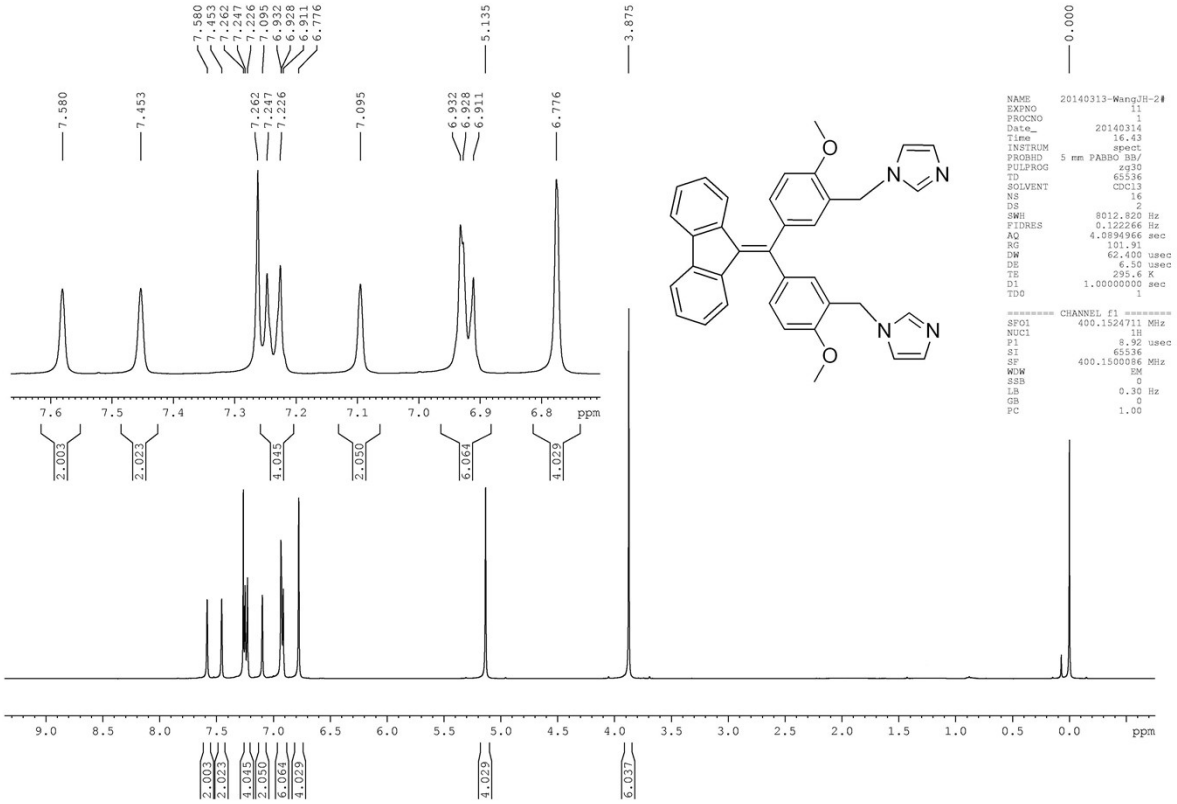

Fig. S1. ^{1}H NMR of diimidazole **8** in $CDCl_3$.

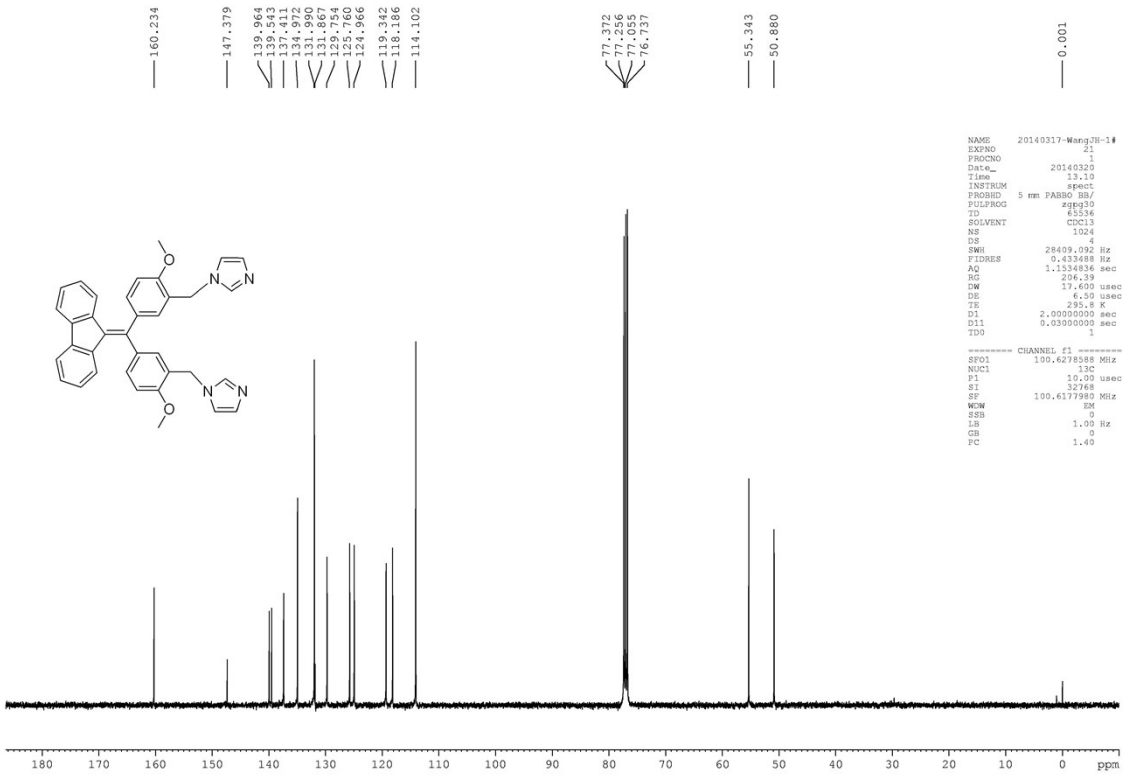

Fig. S2. ^{13}C NMR of diimidazole **8** in $CDCl_3$.

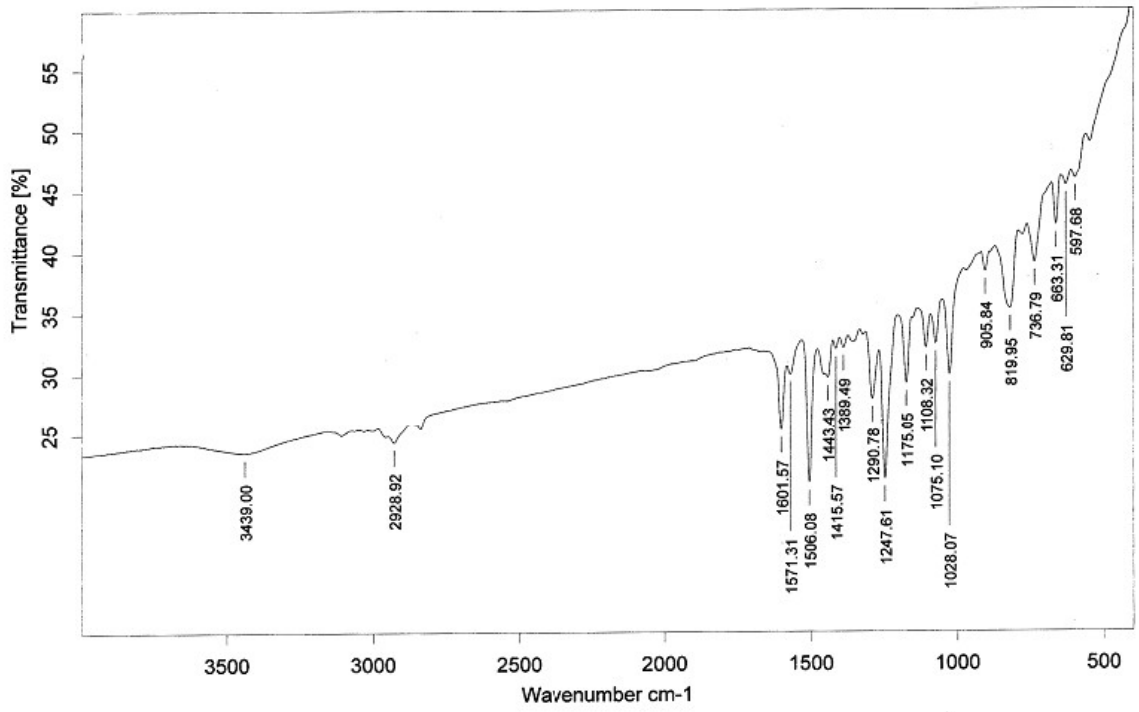

Fig. S3. IR spectrum of diimidazole **8**.

Acquisition Parameter

Source Type	ESI	Ion Polarity	Positive	Set Nebulizer	0.3 Bar
Focus	Active			Set Dry Heater	180 °C
Scan Begin	50 m/z	Set Capillary	4500 V	Set Dry Gas	4.0 l/min
Scan End	3000 m/z	Set End Plate Offset	-500 V	Set Divert Valve	Waste

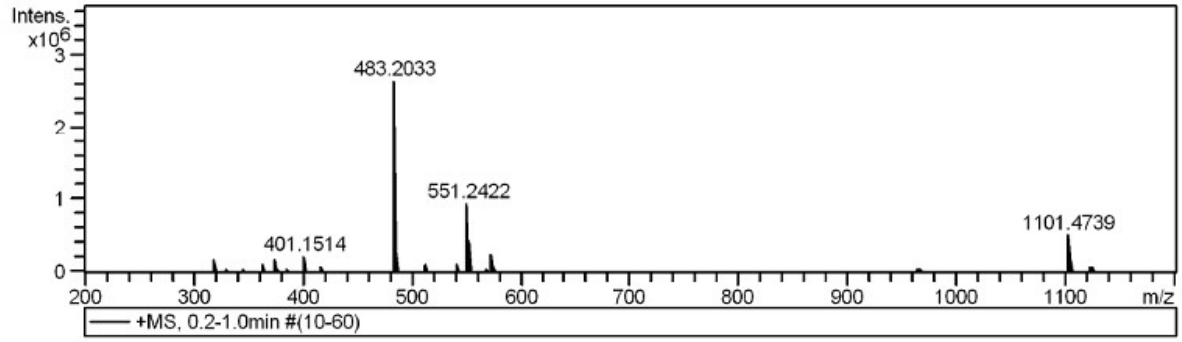

#	m/z	Res.	S/N	I	FWHM
1	318.2981	15301	1011.3	186672	0.0208
2	362.3242	12613	493.0	106210	0.0287
3	375.1300	14749	853.0	191925	0.0254
4	401.1514	13083	913.1	223173	0.0307
5	416.1744	13788	329.7	84284	0.0302
6	483.2033	14341	8658.7	2646627	0.0337
7	551.2422	15062	2854.5	941701	0.0366
8	573.2232	15595	816.2	246315	0.0368
9	966.4442	14645	279.2	27894	0.0660
10	1101.4739	19307	3455.8	512196	0.0571
11	1123.4535	15886	593.0	92557	0.0707

Fig. S4.HRMS spectrum of diimidazole **8**.

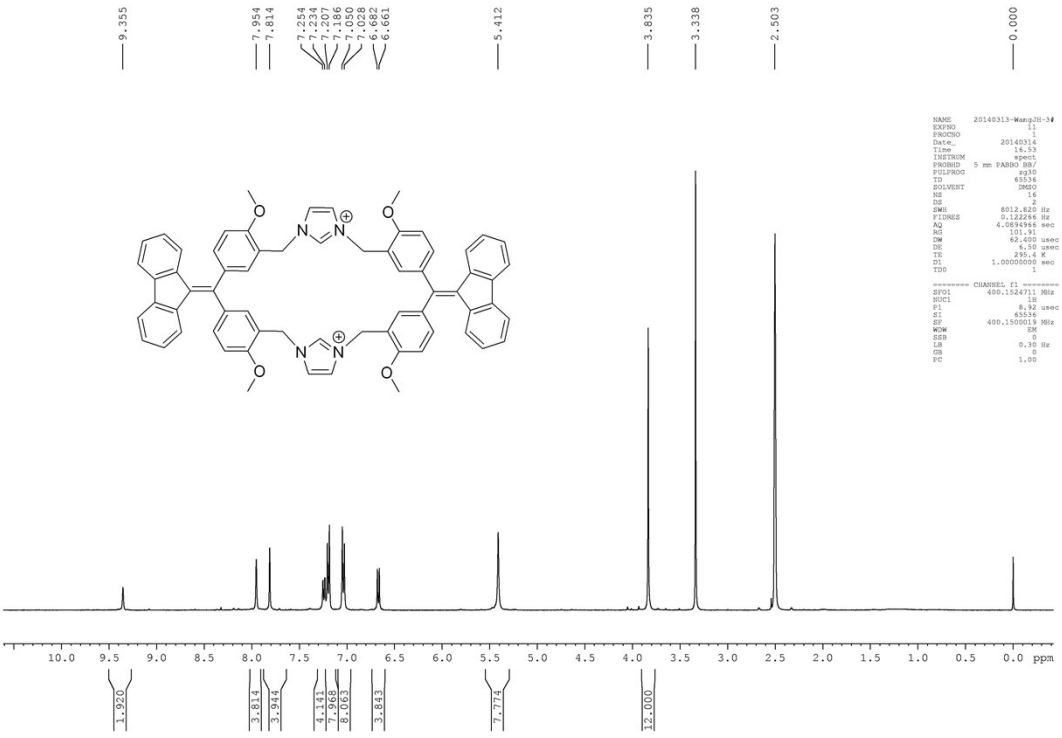

Fig. S5. ^{1}H NMR of the imidazolium macrocycle **1** in DMSO-d_6.

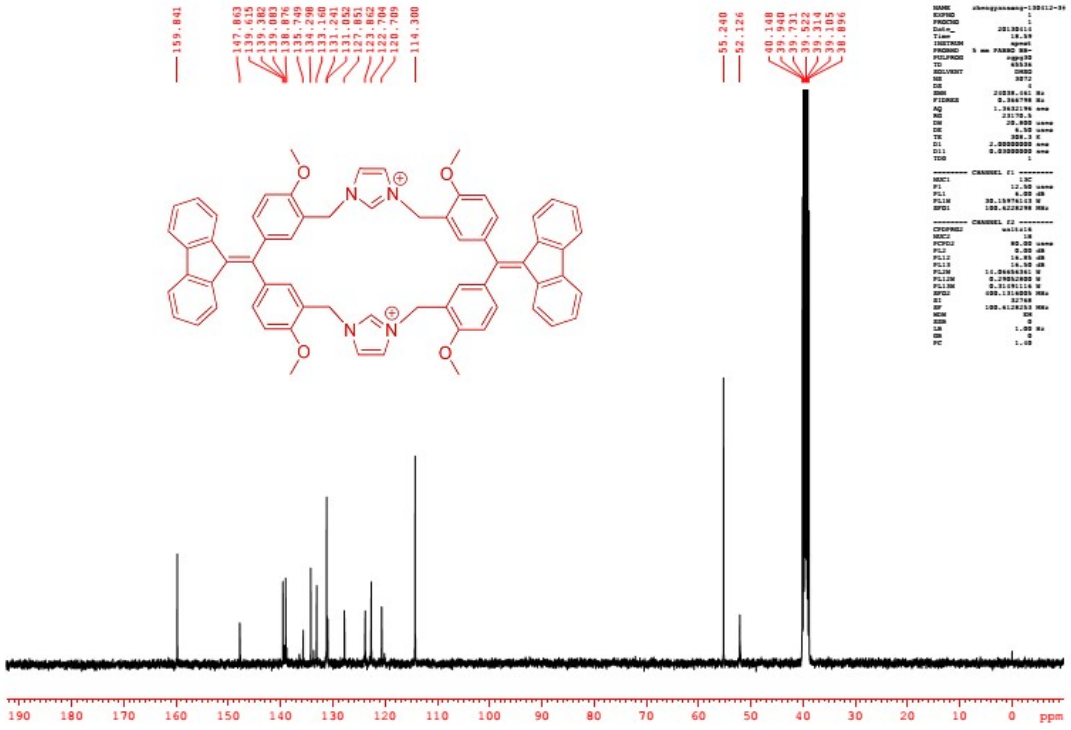

Fig. S6. ^{13}C NMR of the imidazolium macrocycle **1** in DMSO-d_6.

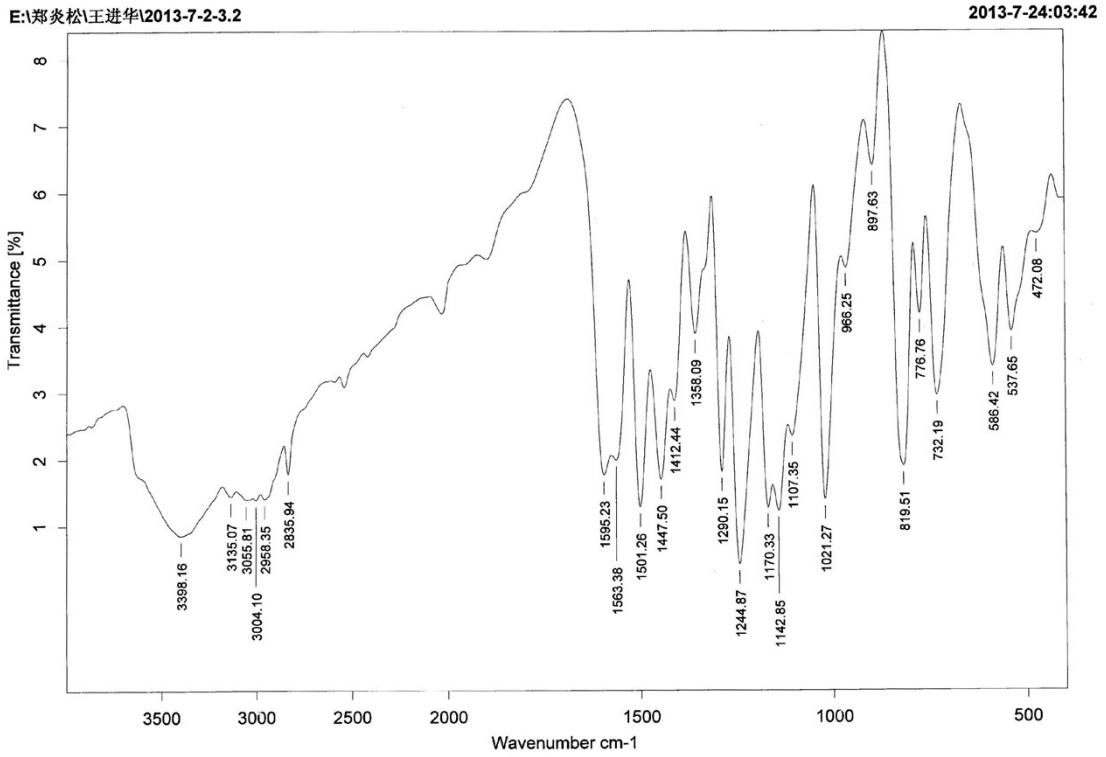

Fig. S7. IR spectrum of the imidazolium macrocycle **1**.

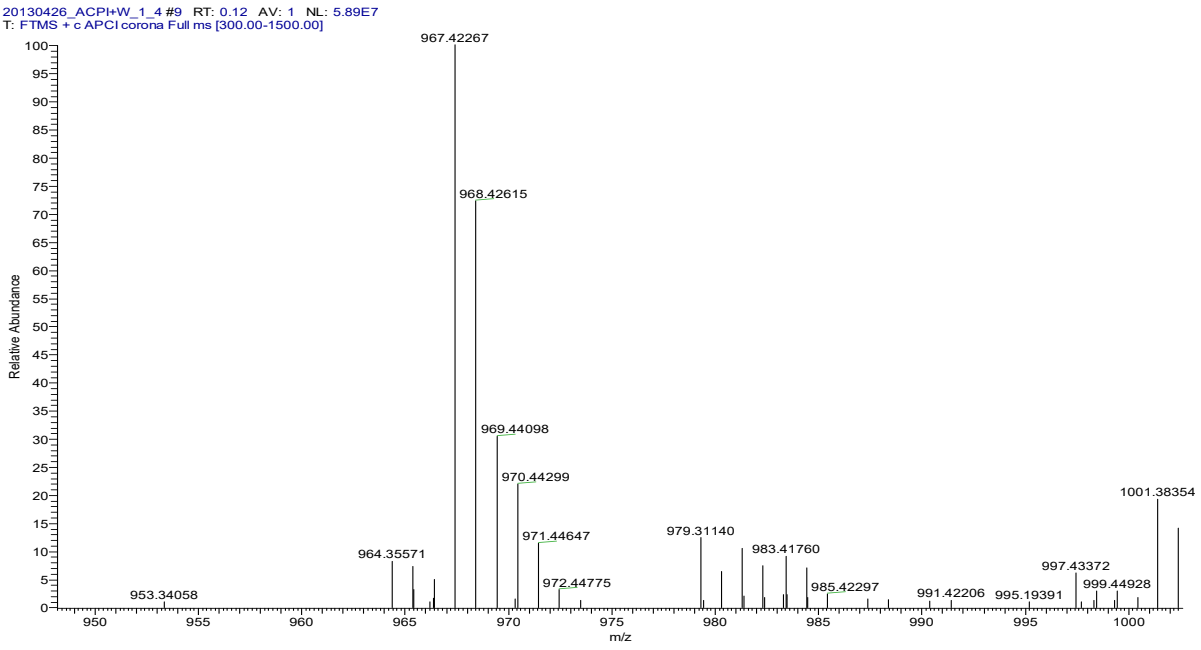

Fig. S8. HRMS spectrum of the imidazolium macrocycle **1**.

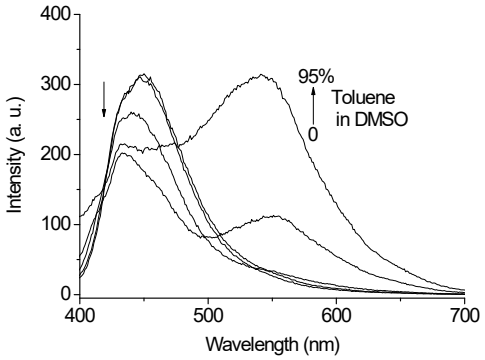

Fig. S9. Change of the fluorescence spectra of **1** with volume percentage of toluene in DMSO. [**1**] = 1.0 × 10^{-5} M, volume percentage of toluene in DMSO: 0, 20, 70, 90, and 95; λ_{ex} = 378 nm, ex/em slits = 5/10 nm.

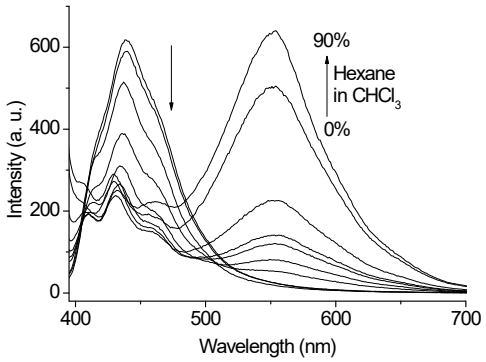

Fig. S10. Change of the fluorescence spectra of **1** with hexane fraction in $CHCl_3$ containing 2% DMSO. [**1**] = 1.0 × 10^{-5} M, λ_{ex} = 378 nm, ex/em slits = 5/10 nm.

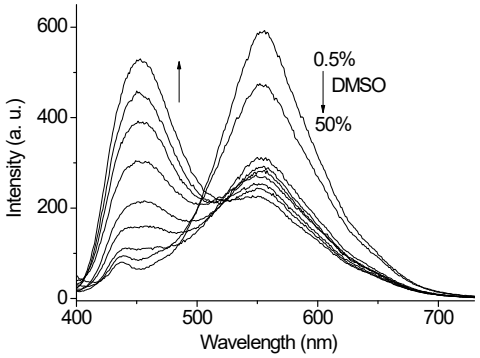

Fig. S11. Change of the fluorescence spectra of **1** with DMSO fraction in H_2O. [**1**] = 2.5 × 10^{-5} M, λ_{ex} = 378 nm, ex/em slits = 10/10 nm.

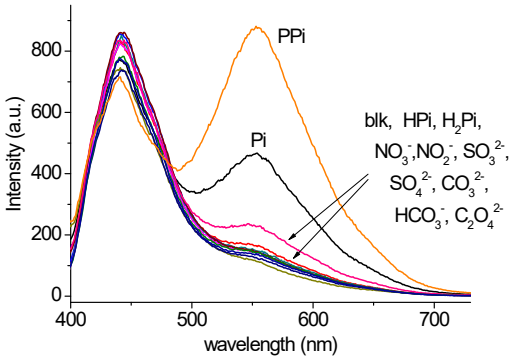

Fig. S12. The fluorescence spectra of **1** in water containing 50% DMSO with addition of different anions. λ_{ex} = 378 nm, ex/em slits = 5/10 nm. [**1**] = 1/2[Anion] = 5.0×10^{-5} M.

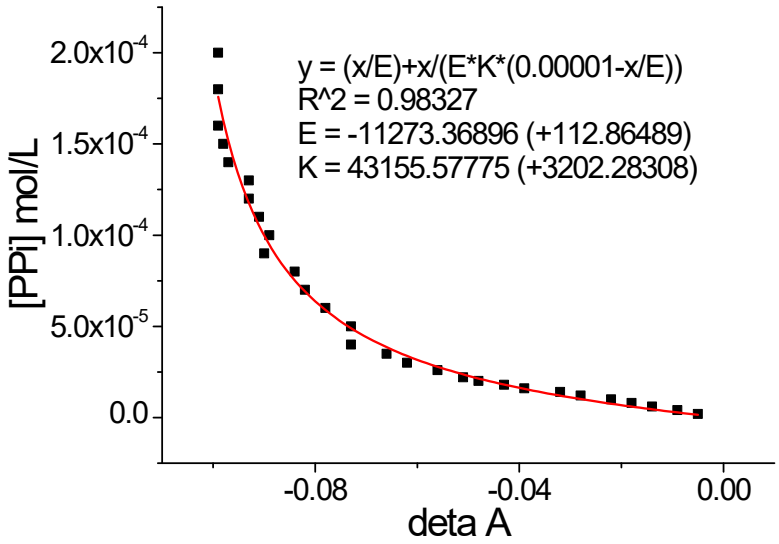

Fig. S13. Change of absorbance difference at 253 nm with concentration of ppi. The red curve is the result from fitting.

Mass Spectrum List Report

Analysis Info

Analysis Name	D:\Data\ZhengYS\zheng-wang-20140611-3.d	Acquisition Date	6/11/2014 10:48:55 AM
Method	tune_wide.m	Operator	BDAL@DE
Sample Name	zheng-wang-20140611-3	Instrument / Ser#	micrOTOF 10401
Comment			

Acquisition Parameter

Source Type	ESI	Ion Polarity	Positive	Set Nebulizer	0.3 Bar
Focus	Active			Set Dry Heater	180 °C
Scan Begin	50 m/z	Set Capillary	4500 V	Set Dry Gas	4.0 l/min
Scan End	3000 m/z	Set End Plate Offset	-500 V	Set Divert Valve	Waste

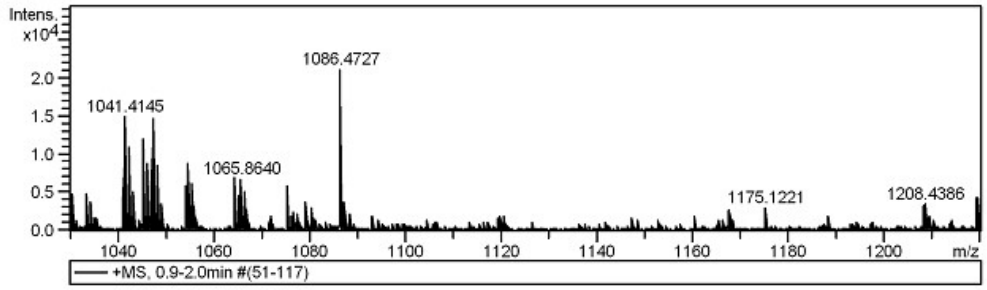

#	m/z	Res.	S/N	I	FWHM
1	1041.4145	15079	115.6	14806	0.0691
2	1042.4187	14384	85.5	10958	0.0725
3	1043.4195	16030	38.3	4912	0.0651
4	1065.3651	15861	34.0	4399	0.0672
5	1065.8640	16513	51.6	6678	0.0645
6	1066.3692	16930	39.0	5052	0.0630
7	1086.4727	11115	161.0	21038	0.0977
8	1087.4108	11656	28.6	3738	0.0933
9	1140.4752	13128	5.7	749	0.0869
10	1141.9834	12642	6.6	875	0.0903
11	1147.4756	11809	10.4	1372	0.0972
12	1148.4435	14456	9.4	1235	0.0794
13	1152.9777	11561	8.7	1147	0.0997
14	1157.4546	14210	4.3	558	0.0815
15	1160.4683	12867	13.5	1763	0.0902
16	1165.3382	15754	10.3	1347	0.0740
17	1166.4303	12453	9.8	1279	0.0937
18	1167.7945	12847	19.9	2599	0.0909
19	1168.4551	11967	9.4	1228	0.0976
20	1175.1221	13022	21.9	2844	0.0902
21	1188.4286	11344	14.4	1859	0.1048
22	1193.1221	12980	4.3	554	0.0919
23	1193.5953	18173	5.2	665	0.0657
24	1194.4550	11729	7.5	966	0.1018
25	1197.4390	12183	8.1	1043	0.0983
26	1202.9580	12394	3.5	450	0.0971
27	1208.4386	11992	25.9	3310	0.1008
28	1209.2904	14819	13.2	1690	0.0816

Fig. S14. ESI+ TOF HRMS of compound **1** in the presence of ppi anion. Multiple peaks observed for the 1:1 complex of [**1**-ppi], such as $[M\text{-}PPi+3Na^+]^+$ $C_{66}H_{54}N_4Na_3O_{11}P_2$ 1209.2957 found 1209.2904 and $[M\text{-}PPi+2H^+\text{+}Na^+]^+$ $C_{66}H_{56}N_4NaO_{11}P_2$ 1165.3319 found 1165.3382. The observed molecular mass of the 1:1 complex of [**1**-ppi] indicate its formation.

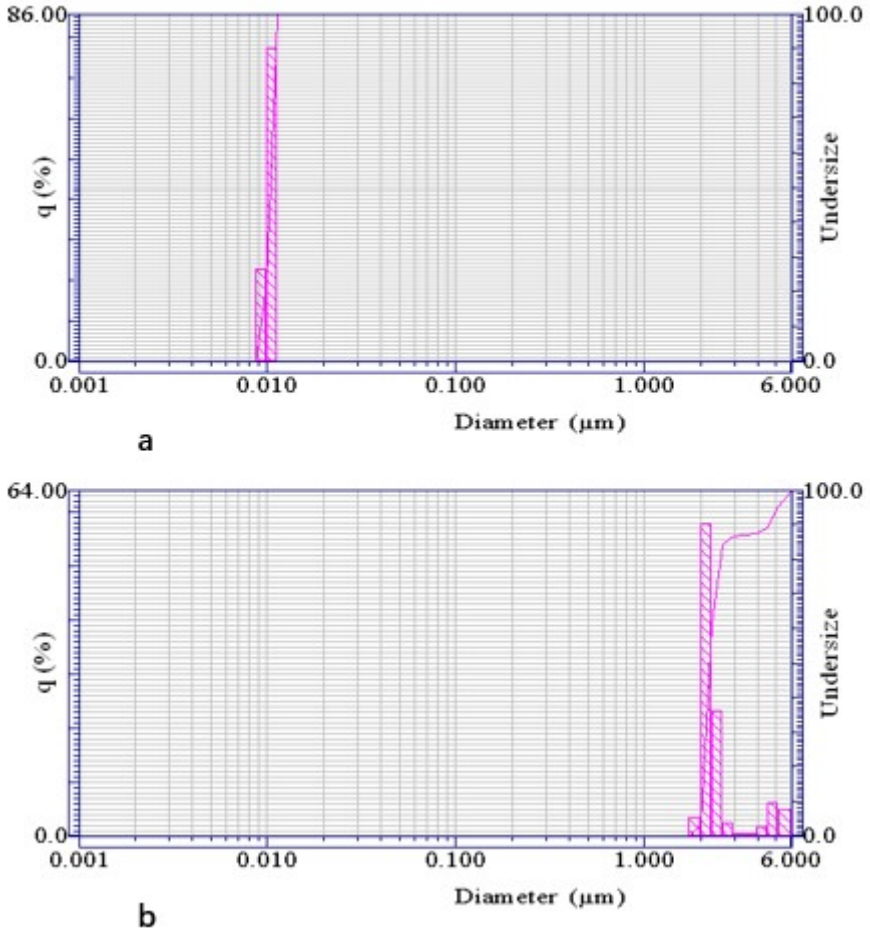

Fig. S15. dynamic light scattering (DLS) measurement: (a) compound **1** with addition of ppi anion without the presence of Zn (II) as reference, 0.0103 µm sized aggregates detected, (b) compound **1** with addition of ppi anion in the presence of Zn (II), 2.5714 µm sized aggregates detected which indicate that large aggregates formed in the presence of Zn (II), without the presence of Zn (II), no significant aggregates formed.

Analytes	Methods	Reference	Detection limit (nM)
PPi	Fluorescence	Chemical communications, 48(2012), 1784-1786	Compound**1**/**2**=1260/2020 nM
	Fluorescence	Analytica Chimica Acta, 1034(2018), 119-127	42 nM
	Fluorescence	Dyes and Pigments, 166(2019), 233–238	Compound**1**/**2**/**3**/**4**/**5**= 13.5/22.2/103/184/198 nM
	Fluorescence	Dyes and Pigments, 168 (2019), 205–211	72.2 nM
	Fluorescence	Dyes and Pigments, 181(2020). 108553	Compound**1**/**2**=22.3nM /113 nM
	Fluorescence	Spectrochimica Acta Part A: Molecular and Biomolecular Spectroscopy, 247(2021), 119073.	320 nM
	Fluorescence	This work	67 nM

Table S1: comparison of detection for ppi with literature reports of similar probes:

Note 1: more discussion of the mechanism

The mechanism for the sensing of pyrophosphate anion with probe **1** is further discussed below. The macrocycle **1**, which bear 2 positive charges, has high affinity towards negatively charged anions through electrostatic attraction. Macrocycle **1** has a cavity of size around 6 Å based on a crystal structure of similar macrocycle reported before (reference 9c, RSC Adv., **2015**, *5*, 60096–60100). The size of cavity of **1** matches very well with the size of pyrophosphate anion (around 5.4 Å). The size fitness between **1** and pyrophosphate anion allow strong binding between **1** and pyrophosphate anion, which has been shown by UV-titration and HRMS analysis. However, this 1:1 association complex has very similar solubility as the probe **1** itself. The fluorescence of **1**, similar as many other compounds with aggregation induced emission characteristics, changes its emission upon formation of aggregates. In here, the inclusion complex [**1**-ppi] does not change much of the solubility which means no significant aggregates are formed. The formation of aggregates, however, could be caused by coordination with Zn (II). The pyrophosphate anion, although included into the cavity of macrocycle **1**, still have the ability to coordinated with Zn (II). This coordination with Zn (II) significantly changed the solubility of the resulting complexes, i.e. formation of aggregates, and hence changed the emission. The formation of aggregation by Zn (II), however, could be many folds. One possibility is that an irregular polymer like coordination complexes formed which naturally leads to large aggregates. Second possibility is that defined complexes formed between Zn (II) and [**1**-ppi], such as (**1**-ppi) Zn, which have low solubility because of charge neutralization.